Surface & Coatings Technology 202 (2008) 5646–5649

Contents lists available at ScienceDirect

Surface & Coatings Technology

journal homepage: www.elsevier.com/locate/surfcoat

Top-emitting organic light-emitting diodes based on semitransparent conducting cathode of Ba/Al/ITO

J.T. Lim, J.H. Lee, J.K. Park, B.J. Park, G.Y. Yeom *

School of Advanced Materials Science and Engineering, SungKyunKwan University, Suwon, Kyunggi-do 440-746, Republic of Korea

ARTICLE INFO

Available online 9 June 2008

PACS:
81.15.J
72.80.L

Keywords:
Top emission
OLEDs
Barium
Semitransparent conducting cathode
Work function

ABSTRACT

Top-emitting organic light-emitting diodes (TEOLEDs) with a thin semitransparent conducting cathode (STCC) of Ba/Al/ITO were fabricated and their electrical/optical characteristics were investigated. At the wavelength of 519 nm, optical properties of STCC of the Ba (5 nm)/Al (10 nm)/ITO (100 nm) structure showed the transmittance of 75% and the reflectance of 13%. The light out-coupling properties of the TEOLED, which is consisted of glass/Ag (100 nm)/ITO (125 nm)/4,4′,4″-tris[2-naphthylphenyl-1-phenylamino]triphenylamine (2-TNATA, 30 nm)/4,4′-bis[*N*-(1-napthyl)-*N*-phenyl-amino]-biphenyl (NPB, 18 nm)/tris(8-quinolinolato) aluminum (III) (Alq_3, 62 nm)/Ba (*x* nm, *x* = 15, 10, and 5 nm)/Al (10 nm)/ITO (100 nm), was increased as the deposition thickness of Ba is reduced. This driving performance of the devices could be interpreted on the base of carrier injection barrier by Fowler–Nordheim tunneling theory as well as the optical properties of the cathode. A constant barrier height of 0.4 eV was obtained for all the devices regardless of the cathode structure composed of Ba (*x* nm)/Al (10 nm)/ITO (100 nm), which indicates the electron-only devices where the injection barrier is at the ITO/2-TNATA interface.

1. Introduction

Organic light-emitting diode (OLED) displays have been recognized in recent years as one of the promising flat panel display (FPD) technologies that are capable of meeting the demand of future information-display application and lighting. Top-emitting (TE) OLED structures coupled with a low temperature poly-silicon (LTPS) thin film transistor (TFT) backplane is one of the most important key-element techniques in active-matrix (AM) OLED displays. This is because the TEOLED cannot only provide a higher aperture ratio than the general bottom-emitting (BE) diodes but also can realize higher image quality on account of its geometrical merit allowing a high pixel resolution [1,2].

In TEOLEDs, semitransparent top cathodes (STCC) play an important role in achieving good device performance. This STCC should satisfy two conflicting requirements simultaneously, i.e. high electrical conductivity and high optical transmittance, to maintain the characteristics of an intrinsic top emission. Moreover, for efficient electron injection from the cathode into the electron-injecting layer (ETL) such as Alq_3 (LUMO level: 3.1 eV), alkali metal (e.g., Cs (2.1 eV) and Li (2.9 eV)) and alkaline-earth metal (e.g., Ca (2.9 eV) and Mg (3.7 eV)) with a low work function have been mainly used as an adjoining cathode layer adjacent to ETL.

Many attempts have been made to develop proper top cathodes [2–9]. Particular attention has been focused on the development of new cathode systems such as semitransparent conducting buffer layers (STCBL)/transparent conducting oxides (TCOs) [e.g., Ag-doped Mg/tin-doped indium oxide (ITO) [6] and Ca/ITO [7]], multi-metal cathode systems [e.g., Ca/Ag [8] and LiF/Al/Ag [9]], and metal-free cathode systems [e.g., copper phthalocyanine (CuPc)/ITO [3] and Li-doped 2,9-dimethyl-4,7-diphenyl-1,10-phenanthroline (BCP)/ITO [2], Cs-doped 4,7-diphenyl-1,10-phenanthroline (Bphen)/Ag [10]]. The multi-metal layers used as cathode systems have been utilized to prevent physical/chemical damage to the organic layers occurring during sputter deposition of the transparent conducting oxides (TCOs) such as ITO in TEOLEDs.

Among the various cathode structures, thin film cathode composed of Ba/Al has been used for an efficient electron injection layer in transitional polymer light-emitting devices [11]. However, TEOLEDs employing Ba/Al as STCC have not been reported to date. In this study, the light out-coupling properties of a TEOLEDs with Ba (*x* nm, *x* = 15, 10, 5, 0 nm)/Al (10 nm)/ITO (100 nm) were investigated in addition to the optical properties of the multilayer cathode and the injection barrier characteristics derived by Fowler–Nordheim tunneling theory.

2. Experimental details

2.1. Device fabrication

Device structure of the TEOLED was composed of glass/Ag (100 nm)/ITO (125 nm, about 10 Ω/□)/2-TNATA (30 nm)/NPB (18 nm)/Alq_3 (62 nm)/Ba (*x* nm, *x* = 15, 10, 5 and 0 nm)/Al (10 nm)/

* Corresponding author.
E-mail address: gyyeom@skku.edu (G.Y. Yeom).

0257-8972/$ – see front matter © 2008 Elsevier B.V. All rights reserved.
doi:10.1016/j.surfcoat.2008.06.036

ITO (100 nm). The Ba thickness of device 1, device 2, device 3 and device 4 was 15, 10, 5 and 0 nm, respectively.

A 100 nm-thick Ag layer consisting of a multilayer anode (Ag/ITO) was vacuum-evaporated on a glass substrate by using a thermal evaporator. Onto this Ag layer, a 125 nm-thick ITO layer was deposited by conventional dc sputtering, followed by a heat treatment; the ITO deposition was carried out in Ar at the pressure of 5 mTorr mixed with less than 2% O_2 at the dc power of 400 W. Organic layers (2-TNATA/NPB/Alq_3) consisting of 30 nm-thick 4,4′,4″-tris(2-naphthylphenyl-1-phenylamino)triphenylamine (2-TNATA) as a hole-injecting layer (HIL), 18 nm-thick 4,4′-bis(*N*-(1-napthyl)-*N*-phenyl-amino)-biphenyl (NPB) as a hole-transporting layer (HTL), and 62 nm-thick tris(8-quinolinolato)aluminum(III) (Alq_3) as an electron-transporting layer (EIL) were sequentially deposited by using a thermal evaporator system. The *x* nm-thick Ba layer and a 10 nm-thick Al layer consisting of a multilayer cathode (Ba/Al/ITO) were deposited onto the multi-organic layers by using a thermal evaporator. Finally, the 100 nm-thick ITO capping layer was deposited by dc sputtering in Ar at the pressure of 5 mTorr mixed with O_2 at a power of 100 W. The emissive active area of the devices was 1.4×1.4 mm^2.

2.2. Measurement

Reflectance spectra and transmittance spectra of the electrodes were measured by using a UV–VIS–NIR spectrophotometer with a VW specular wavelength reflectance (Cary 5000 UV/VIS/NIR, Varian Inc.) and a UV spectrophotometer (UV S-2100, SCINCO Inc.) in air, respectively. The resistivity was measured by using a four-point probe (CMT-SERIES, CHANG MIN Co. Ltd.). The current–voltage–luminance characteristics were measured using a source-measure unit (2400, Keithley Instrument Inc.) while the emission intensities from the TEOLEDs devices were measured by using the photocurrent induced on a silicon photodiode (Oriel 71608) with a picoammeter (485, Keithley Instrument Inc.). The electroluminescence (EL) spectra of the as-fabricated devices were measured by using optical emission spectroscopy (PCM-420, SC Tech. Inc.).

3. Results and discussion

To inject an electron efficiently, the introduction of Ba having low work function between an adjoining cathode layer adjacent to Alq_3 and the Alq_3 layer could be expected to reduce the electron injection barrier. Therefore, the use of Ba with a low work function of 2.7 eV could lead to a device performance with efficient electron injection. Meanwhile, Al in the Ba/Al/ITO cathode is used as a protecting layer to prevent the oxidation of both Ba and the organic layers, which are sensitive to atmospheric moisture and oxygen. A thin layer of Al has a relatively low optical absorption and the highest conductivity among metals. In addition, ITO (refractive index: 1.95) [12] was used as a high-refractive-index-matching layer for the enhancement of the optical transmission through the top of the device and as a semi-passivation layer to protect the device. As the anode of the TEOLED, high reflectivity as a mirror and proper cavity property are required to achieve a strong radiative emission as the electric field of states is proportional to the reflectivity of the mirrors and to the reciprocal of the length of the cavity [12]. To obtain a high light-output in this TEOLED study, Ag/ITO was used as a highly reflective anode system with a good electrical conductivity, and Ba/Al/ITO was introduced as a highly transmittable cathode system with a good conductivity.

During the deposition of ITO onto glass/Ag/ITO/organic layers/Ba/Al, if the thickness of Ba/Al cathode system is not thick enough, the device could be damaged by the plasma through oxidation and physical damage of the organic layers. In fact, the TEOLED with the Ba (*x* nm)/Al (10 nm) (below 15 nm in total thickness) cathode showed a poor device performance after the sputter deposition of the 100 nm-thick ITO capping layer (not shown). Therefore, the Ba (*x* nm)/Al (10 nm) cathode system having the total thickness between 15 and 25 nm was used in this study, to prevent both physical damage of the organic layers and the oxidation of Ba during the ITO deposition.

Fig. 1(a) and (b) shows the transmittance curves and the reflective curves, respectively, as a function of wavelength for Ba (*x* nm: *x*=0–15)/Al (10 nm)/ITO (100 nm). Although the transmittance of cathode is largely decreased with increasing the Ba thickness in the glass/Ba (*x* nm)/Al (10 nm)/ITO (100 nm) cathode, in the view of a transmittance uniformity, the cathode structure composed of glass/Ba (5 nm)/Al (10 nm)/ITO (100 nm) exhibited the most flat property in the range of 70–78% at the wavelength of 450–650 nm among the cathode structures. In the case of the reflective curves shown in Fig. 1(b), the structure of glass/Ba (5 nm)/Al (10 nm)/ITO (100 nm) also showed the most flat property in the range of 14–15%. If the cathode structure does not show flat optical property such as glass/Al (10 nm)/ITO (100 nm), it can exhibit a limitation in a top emission configuration. Therefore, the structure of glass/Ba (5 nm)/Al (10 nm)/ITO (100 nm) showed the optimum condition having the transmittance of 75% and the reflectance of 13% at the maximum wavelength (519 nm) of the electroluminescent (EL) spectrum. In addition, when the thickness of Ba in Ba (*x* nm)/Al (10 nm)/ITO (100 nm) cathode is 15, 10, 5 and 0 nm, resistivities of the multilayer cathode are 0.85, 1.16, 1.13, and 1.03×10^{-3} Ω·cm, respectively. Also, the Ag (100 nm)/ITO (125 nm) anode shows a resistivity of about 4.0×10^{-6} Ω·cm. Here, the difference of resistivity is estimated to occur by the difference of the interfacial geometry structure between Ba and Ag.

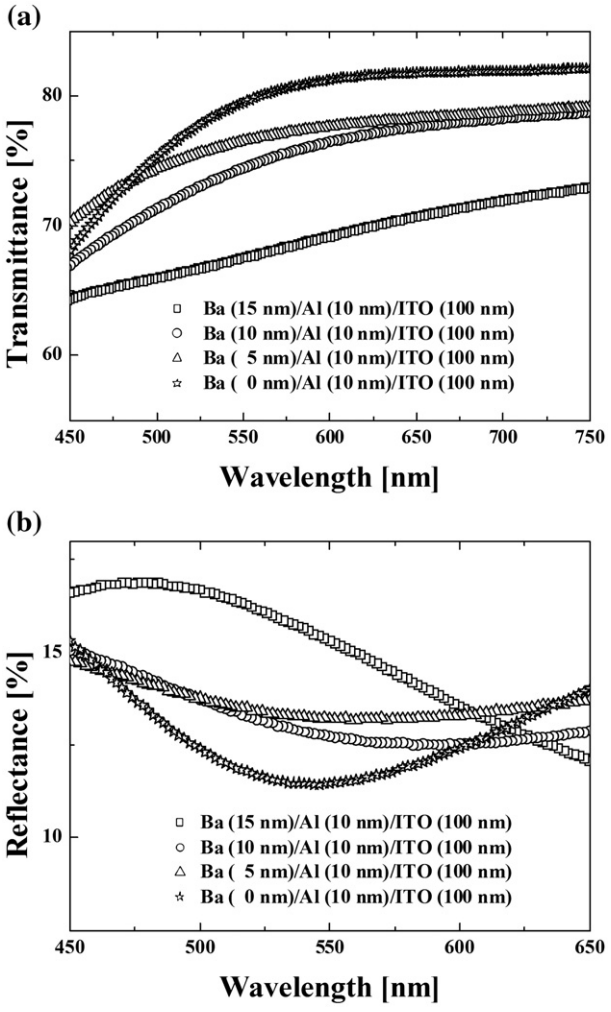

Fig. 1. (a) Transmittance and (b) reflectance spectra of Ba/Al/ITO as a function of the wavelength for glass/Ba (*x* nm)/Al (10 nm)/ITO (100 nm) (*x*=15, 10, 5, 0 nm).

Using the TEOLEDs fabricated with the cathode system and the anode system described above, the current–voltage–luminance characteristics of the devices (Ba thickness in Ba/Al (10 nm)/ITO (100 nm); device 1, 2, 3, 4 = 15, 10, 5, 0 nm) were measured and the results are shown in Fig. 2(a). The current density–voltage–luminance characteristics and the EL characteristic for devices 1–3 are also summarized in Table 1. Turn-on voltages (V_T) for device 1, device 2, device 3 and device 4 were 7.6 2.8, 2.6, 2.6, and 5.0 V, respectively. As shown in Fig. 2(a) and Table 1, at a luminance of about 100 cd/m^2 (L_{100}), the current densities (J) of device 1, device 2 and device 3 were 22 mA/cm^2 (7.6 V), 25 mA/cm^2 (6.6 V), and 25 mA/cm^2 cm^2 (6.2 V), respectively. The maximum luminances (L_{max}) for devices 1–3 were 11,800 (15.2 V), 23,300 (14.0 V), and 43,400 cd/m^2 (13.4 V), respectively, as shown in Table 1. Fig. 2(b) shows the external quantum efficiency (η_{ext}) and the power efficiency (η_{PE}) for devices 1–3 as a function of the luminance, and the results are also summarized in Table 1, As shown in Fig. 2(b) and Table 1, η_{PE} at L_{100} for devices 1–3 were 1.7, 1.9 and 2.6%, respectively, and η_{ext} at L_{100} were 1.3, 1.5, and 1.9 lm/W, respectively. When the characteristics of the devices such as V_T, J, L_{max}, η_{ext}, and η_{PE} were compared, device 3 having the cathode structure of Ba (5 nm)/Al (10 nm)/ITO (100 nm) showed the most excellent driving performance. Data based on the current density–voltage–luminance characteristics exhibits that the light out-coupling efficiency is largely dependent on the optical property shown in Fig. 1. Therefore, the most excellent driving performance of device 3 is attributed to the improved aperture ratio by the high transmittance and electrical conductivity of the Ba (5 nm)/Al (10 nm)/ITO (100 nm).

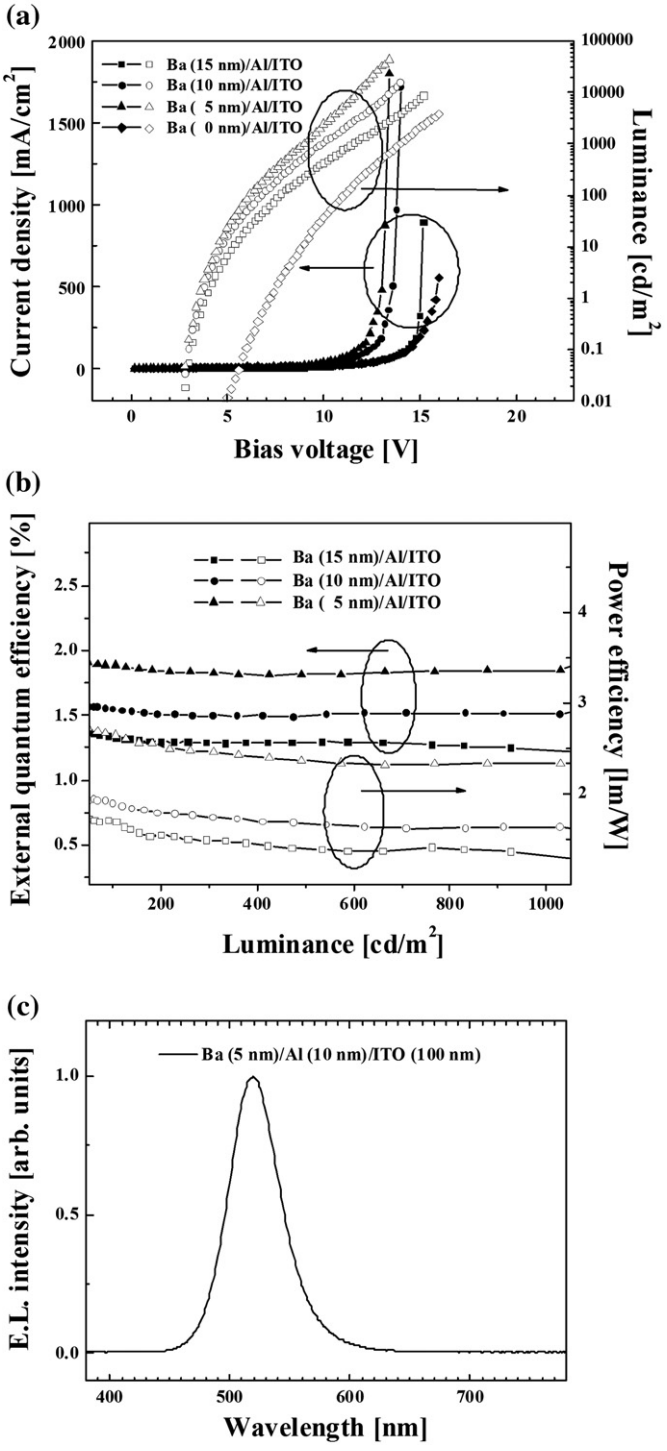

Fig. 2. (a) Current density and luminance curves as a function of bias voltage. (b) External quantum efficiency and power efficiency as a function of a luminance. (c) EL spectrum for device 3. Devices were composed of glass/Ag (100 nm)/ITO (125 nm)/2-TNATA (30 nm)/NPB (18 nm)/Alq$_3$ (62 nm)/Ba (x nm)/Al (10 nm)/ITO (100 nm) (Ba thickness of devices 1, 2, 3, 4 = 15, 10, 5, 0 nm).

Table 1
Current density–voltage–luminance characteristics and the electroluminescent properties of the devices composed of glass/Ag (100 nm)/ITO (125 nm)/2-TNATA (30 nm)/NPB (18 nm)/Alq$_3$ (62 nm)/Ba (x nm)/Al (10 nm)/ITO (100 nm) (Ba thickness of devices 1, 2, 3, 4 = 15, 10, 5, 0 nm)

Device	Thickness of Ba/Al [nm]	EL λ_{max}[a] [nm]	η_L at 100 cd/m^2 [lm/W]	η_{ext} at 100 cd/m^2 [%]	L_{max} [cd/m^2]	V at 100 cd/m^2 [V]	Barrier height[b]
1	15/10	–	1.7	1.3	11,800 at 15.2 V	7.6 at 22 mA/cm^2	0.41
2	10/10	–	1.9	1.5	23,300 at 14.0 V	6.6 at 25 mA/cm^2	0.44
3	5/10	519	2.6	1.9	43,400 at 13.4 V	6.2 at 25 mA/cm^2	0.36

[a] The maximum EL peaks at the luminance of 100 cd/m^2.
[b] Values calculated by Fowler–Nordheim equation.

Fig. 2(c) shows the EL spectrum for device 3 measured at the normal viewing angle and at L_{100}. As shown in Fig. 2(c), the maximum EL peak was found at a wavelength of 519 nm. The maximum EL peak of 519 nm was obtained by adjusting the macro-cavity effect [13], which could be controlled by changing the thickness of ITO composing the multilayer anode.

Meanwhile, the carrier injection from the electrode to organic layers (ETL or HIL) of the devices can be understood by measuring the barrier height. Barrier height for the carrier injection was analyzed through the Fowler–Nordheim tunneling theory [14]. Fowler–Nordheim (F–N) equation can be expressed as follows;

$$I \propto F^2 \exp\left(\frac{-k}{F}\right), \tag{1}$$

where, I is the current, F is the electric-field strength, and k is a parameter that depends on the barrier shape. Fig. 3(a) shows a plot of $In(I/F^2)$ vs $1/F$ for device 3 with 110 nm-thick organic layer. The plot is close to linear, particularly above the operating voltage. If it is assumed that the injected charge is tunneled through a triangle barrier at one of the interfaces, the constant k in Eq. (1) is given by

$$k = \frac{8\pi\sqrt{2m^*}\varphi^{3/2}}{3qh}. \tag{2}$$

here, φ is the barrier height, and m^* is the effective mass. Table 1 also shows the values of barrier height of devices 1–3 calculated by the F–N equation by assuming that the electric field is constant across the

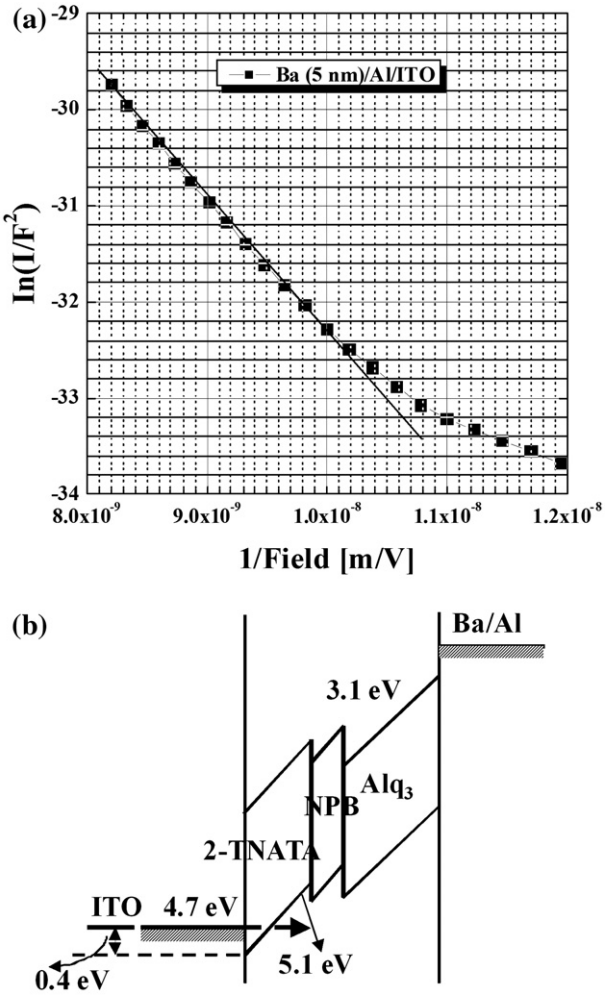

Fig. 3. (a) Fowler–Nordheim plot for a device composed of Ag (100 nm)/ITO (125 nm)/2-TNATA (30 nm)/NPB (18 nm)/Alq_3 (62 nm)/Ba (5 nm)/Al (10 nm)/ITO (100 nm). (b) Proposed energy band diagram for electron-only device with Ba/Al/ITO cathode.

device and the effective mass equals to free electron mass. These data indicate a constant barrier height of 0.4 eV for devices 1–3 containing Ba. Ref. [15] shows that the difference of work function between the Alq_3 layer and the Ba-on-Alq_3 interfaces for the Ba thickness from 5 to 15 nm was not as high as 0.4 eV and was varied with Ba thickness (not shown). The barrier height is independent of the Ba/Alq_3 cathode structure used in this study and it must be at the ITO/2-TNATA interface of anode, because the structure of the organic layers and anode was maintained the same. This explains that the TEOLEDs with the Ba/Al/ITO cathode are the electron-only devices which are independent of the work function of the cathode. Meanwhile, the bipolar current of a hole and electron current is contributed to the current in the electric field of Fig. 3(a). Here, an electron functions as a majority carrier and a hole roles as a minority carrier. Fig. 3(b) exhibits the proposed band diagram of the electron-only devices. The barrier height of 0.4 eV for carrier injection is estimated to occur when a hole is injected from the ITO (4.7 eV) layer [16] to the 2-TNATA (5.1 eV) layer [17].

4. Conclusions

At the wavelength of 519 nm, a STCC with 5 nm-thick Ba in the Ba (x nm)/Al (10 nm)/ITO (100 nm) (x=5, 10, and 15 nm) structure showed the highest transmittance of 75% and the proper reflectance of 13%. In the case of a STCC with a low reflectance of below 15%, when a light emitted from the emissive layer propagates cross a STCC, the EL wavelength might mainly depend on the transmittance of STCC rather than the reflectance (STCC) which results in various interference effects in the microcavity structure. Also, the Ba (5 nm)/Al (10 nm)/ITO (100 nm) STCC has the most flat optical property, compared to other devices at the wavelength range between 450 and 650 nm. Meanwhile, the barrier height of carrier injection for all devices was 0.4 eV, regardless of the cathode structure (Ba (x nm)/Al (10 nm)/ITO (100 nm) (x=5–15 nm). This constant barrier height by Fowler–Nordheim tunneling analysis indicates the electron-only device where the injection barrier is at the ITO/2-TNATA. Therefore, the driving performance of the TEOLEDs with the Ba/Al/ITO STCC system used in this study could explain to be dependent on the transmittance rather than the electron injection property of STCCs.

Acknowledgment

This work was supported by National Program for Tera-level Nanodevices of the Korea Ministry of Science and Technology as one of the 21st Century Frontier Programs.

References

[1] S. Miyaguchi, S. Ishizuka, T. Wakimoto, J. Fukuda, H. Kubota, K. Yoshida, T. Watanabe, H. Ochi, T. Sakamoto, M. Tsuchida, I. Oshita, T. Tohma, Extended Abstracts 9th Int. Workshop on Inorganic and Organic Electroluminescence, Bend, OR, September 1998, p. 137.
[2] C. Hosokawa, Synth. Met. 91 (1997) 3.
[3] Z. Shen, P.E. Burrows, V. Bulovic, S.R. Forrest, M.E. Thomson, Science 276 (1997) 2009.
[4] H.-S. Woo, S.J. Cho, T.-W. Kwon, D.-K. Park, Y.-B. Kim, R. Czerw, D.L. Carroll, J.-W. Park, J. Korean Chem. Soc. 46 (2005) 981.
[5] C.W. Tang, S.A. VanSlyke, Appl. Phys. Lett. 51 (1987) 913.
[6] P.S. Bryran, F.V. Lovecchio and S.A. VanSlyke, US Patent No. 5141671, Aug, 25 (1992).
[7] F. Papadimitrakopoulos, X.-M. Zhang, D.L. Thomsen, K.A. Higginson, Chem. Mater. 8 (1996) 1363.
[8] R.C. Kwong, M.R. Nugent, L. Michalski, T. Ngo, K. Rajan, Y.-J. Tung, M.S. Weaver, T.X. Zhou, M. Hack, M.E. Thompson, S.R. Forrest, J.J. Brown, Appl. Phys. Lett. 81 (2002) 162.
[9] L.S. Hung, C.W. Tang, M.G. Mason, P. Raychaudhuri, J. Madathil, Appl. Phys. Lett. 78 (2001) 544.
[10] Q. Huang, K. Walzer, M. Pfeiffer, V. Lyssenko, G. He, K. Leo, Appl. Phys. Lett. 88 (2006) 113515.
[11] Q. Feng, Z.-Y. Lu, Y. Huang, M.-G. Xie, S.-H. Han, J.B. Pong, Y. Cao, Macromolecules 37 (2004) 260.
[12] M.-H. Lu, J.C. Sturn, J. Appl. Phys. 91 (2002) 595.
[13] G. Patharathy, C. Shen, A. Kahn, S.R. Forrest, J. Appl. Phys. 89 (2001) 4986.
[14] I.D. Parker, J. Appl. Phys. 75 (1994) 1656.
[15] In ultraviolet photoemission spectroscopy (UPS) analyses, work function for the interfaces of pristine Alq_3, Ba (50 nm)-on-Alq_3 (100 nm), Ba (100 nm)-on-Alq_3 (100 nm) and Ba (15 nm)-on-Alq_3 were 2.8, 2.9, 2.7 and 2.7, respectively.
[16] G. Partharathy, P.E. Burrows, V. Khalfin, V.G. Kozlov, S.R. Forrest, Appl. Phys. Lett. 72 (1998) 2138.
[17] K. Okumoto, Y. Shirota, J. Lumin. 87–89 (2000) 1171.